Modelling Parameter Role on Accuracy of Cardiac Perfusion Quantification

Niloufar Zarinabad[1,*], Amedeo Chiribiri[1], Gilion L.T.F. Hautvast[2], Andreas Shuster[1], Matthew Sinclair[1], Jeroen P.H.M. van den Wijngaard[3], Nicolas Smith[1], Jos A.E. Spaan[3], Maria Siebes[3], Marcel Breeuwer[4], and Eike Nagel[1]

[1] Division of Imaging Sciences and Biomedical Engineering, Kings College London, St. Thomas Hospital London, UK
{Niloufar.Zarinabad,Amedeo.chiribiri, Andreas.shuster,Matthew.Sinclair, Nicolas.Smith,Eike.Nagel}@kcl.ac.uk
[2] Philips Group Innovation – Healthcare Incubators, Eindhoven, The Netherlands
Gilion.Hautvast@philips.com
[3] Department of Biomedical Engineering & Physics, Academic Medical Centre, Amsterdam, The Netherlands
{J.P.Vandenwijngaard,J.A.Spaan,M.Siebes}@amc.uva.nl
[4] Philips Healthcares, Imaging Systems – MR, Veenpluis 4-6, 5680 DA Best, The Netherlands
Marcel.Breeuwer@philips.com

Abstract. Cardiovascular magnetic resonance (CMR) perfusion data are suitable for quantitative measurement of myocardial blood flow. The goal of perfusion-CMR post- processing is to recover tissue impulse-response from observed signal-intensity curves. While several deconvolution techniques are available for this purpose, all of them use models with varying parameters for the representation of the impulse-response. However this variation influences the accuracy of the deconvolution and introduces possible variations in the results. Using an appropriate order for quantification is essential to allow CMR-perfusion-quantification to develop into a useful clinical tool. The aim of this study was to evaluate the effect of parameter variation in Fermi modelling, autoregressive moving-average model (ARMA), B-spline-basis and exponential-basis deconvolution. Whilst Fermi is the least dependent method on the modelling parameter determination, the B-spline and ARMA were the most sensitive models to this variation. ARMA upon a correct choice of order showed to be the superior to other methods.

Keywords: Perfusion quantification, Deconvolution, Model order.

1 Introduction

First pass cardiac magnetic resonance (CMR) perfusion, is capable of providing a quantitative measurement of myocardial blood flow (MBF) that could yield functional information allowing for a more accurate diagnosis and for optimization of therapy.

* Corresponding author.

S. Ourselin, D. Rueckert, and N. Smith (Eds.): FIMH 2013, LNCS 7945, pp. 370–382, 2013.

Perfusion CMR measures the level of signal intensity which is assumed to be linearly proportional to concentration of a contrast agent,$C_{myo}(t)$, in a myocardial region of interest (ROI)[1, 2]. This concentration depends on perfusion rate and arterial concentration of the agent, $C_{aif}(t)$, which is also acquired in the form of signal intensity in the perfusion CMR process, through a convolution integral

$$C_{myo}(t) = C_{aif}(t) \otimes h(t)$$

where $h(t)$ is the response function of the myocardial ROI and characterizes its perfusion properties(i.e. MBF)[3, 4]. The goal of perfusion MRI post processing is to recover $h(t)$ from observed $C_{aif}(t)$, and $C_{myo}(t)$. The most common technique is to find $h(t)$ through solving a least square minimization problem:

$$min_{h(t)} \left\| C_{myo} - C_{aif}(t) \otimes h(t) \right\|^2$$

This task is challenging because it amounts an ill-posed inverse problem [5-7] and therefore needs regularisation. Several techniques have been used in other studies to solve this ill posed problem and favourable results have been reported [4, 8-14]. These techniques use different strategies to represent tissue impulse response, but a common feature of each of these techniques is dependency of perfusion estimate accuracy on the mathematical model. The mathematical models, utilized for $h(t)$ approximation, use varying parameters. Development of these models consists of several logical steps, one of which is the determination of parameters which are exerting the most influence on the model results.

Although estimating MBF values from the available mathematical models have been reported in several studies, rarely they have investigated the influence of model parameter changes on the outcome of deconvolution.

The purpose of this study was to systematically examine how changes in each model's varying parameter will influence the deconvolution outcome and affect its accuracy and precision. These results are important for the implementation and interpretation of future studies aimed at modelling of the myocardial impulse response.

2 Theory

The mathematical models used here for representation of the $h(t)$ include series of B-spline functions[11], autoregressive moving average model (ARMA)[14], series of exponential functions[7] and Fermi function modelling[12].

2.1 Series of B-spline Functions

Jerosch-Herold et.al[11] developed a model of independent deconvolution approach to estimate myocardial perfusion from tissue impulse response, which parameterized $h(t)$ as a sum of weighted B-spline functions as [11, 15].

$$h(t) = \sum_{j=1}^{P} h_j \, B_j^{(k)}(t)$$

Here the degree of splines (k), the number of splines (P) and the positions of the break points (control points) (h_j) are the varying parameters in the B-spline functions.

In order to keep the inverse problem linear, only the position of control points will be estimated by the least square minimization problem.

2.2 ARMA

The ARMA model assumes that the discrete time samples of measured $C_{myo}(t)$, and $C_{aif}(t)$ are related together according to[10]:

$$C_{myo}(t) = \sum_{i=0}^{Q} b_i C_{aif}(t-i) + \sum_{j=1}^{L} a_j C_{myo}(t-j)$$

in ARMA modelling, the only factors which have influence on the model accuracy are the auto-regressive and moving average order ($Q$and L). Estimation of the ARMA model order requires that the model to be fitted for many L and Q orders to find the smallest values of L and Q which provide an acceptable fit to the data. The value of Q and L should be chosen large enough, not to exclude the efficient model.

2.3 Series of Exponential Basis

Hautvast et.al [16] recently demonstrated that $h(t)$can be parameterized as sum of exponential decaying function and the regularization of the inverse problem can be

$$h(t) = \sum_{m=1}^{M} h_m f_m = \sum_{m=1}^{M} h_m e^{-\lambda_m t}$$

The regularization of this inverse problem can be performed by constraining the estimated kernel to be monotonic. To keep the minimization problem in linear range, the total number of exponential functions (M) and the decay rates of the exponential functions (λ_m) is prefixed and any perturbation will have an effect on the accuracy of the regularization outcome.

2.4 Fermi

Jerosch- Herold et al. [12] and Wilke et al. [17] fitted time curves for tissue impulse response function to the Fermi function with the following analytical expression:

$$h(t) = F.\left[\frac{1}{\exp[(t-\tau_{onset}).kr]+1}\right]\theta(\tau_{onset})$$

using a Marquardt-Levenberg nonlinear least square algorithm by letting kr and F vary and keeping other parameters fixed. In the above equation $\theta(\tau_{onset})$ is the unit step is function and τ_{onset} accounts for the delay between arrival of the contrast agent in LV and myocardium ROI. kr is the decay rate of $h(t)$due to contrast agent washout. As nonlinear least square method has been used for regularization when the Fermi function modelling is used, all of the varying parameters of Fermi function including kr, and F will be calculated from the least square minimization

problem[12]. The only user dependent parameter in Fermi modelling is τ_{onset}, which can be calculated for each ROI using its corresponding SI curves[18].

3 Material and Method

The four approaches - series of B-spline functions, ARMA, series of exponential function and Fermi function modelling were tested on two sets of data. The first set of data was simulated so that there was a known reference to assess the sensitivity of the models to additive noise. The second test of data was acquired from an MR compatible blood perfused pig heart model. For each data set, we have changed the regularization independent parameter of the models in order to find the best parameter which gives the most accurate results.

3.1 Simulated Data

Simulated data allows for the examination of the influence of variation in quantification-method-orders on the perfusion estimates by calculating the absolute error of quantification. The unit step function has been chosen as a noiseless tissue impulse response, $h_{GS}(t)$. $C_{aif}(t)$ used in this experiment is a convolution of many exponentials as suggested in [7] to model the propagation of an impulsive bolus injection through several compartments of the cardiovascular system.

$$C_{aif}(t) = \delta(t) * \left[ve^{-vt}\right]_1 * \left[ve^{-vt}\right]_2 * \ldots * \left[ve^{-vt}\right]_n$$

Initial $C_{myo}(t)$ was then obtained by convolving $h_{GS}(t)$ with the simulated $C_{aif}(t)$ [7]. Finally the constructed $C_{myo}(t)$ and $C_{aif}(t)$ have been corrupted by additive white Gaussian noise with a selected standard deviation.

3.2 Explanted Pig Heart

Experiments were performed using the set up described by Shuster et.al [19]. Perfusion-CMR was performed at rest and during pharmacological vasodilation with adenosine. During adenosine infusion the flow was altered to maintain the same coronary perfusion pressure as during the resting state. The scans (n=5) were performed on a 3 Tesla (Achieva TX, Philips, Best, The Netherlands) clinical MR scanners. We used a saturation recovery gradient echo pulse sequence accelerated with k–t BLAST (k-t factor 5 and 11 training profiles) with a repetition time of 2.7 ms, echo time of 0.9 ms, flip angle 20°, spatial resolution at 1.3 x 1.3 x 8 mm. Perfusion CMR was performed using a dual-bolus scheme with 5 ml of neat (0.07 mmol/ml) and 5 ml of dilute (0.007 mmol/ml) gadobutrolum bolus injections (Gadovist, Bayer Healthcare, Leverkusen, Germany)[20]. Immediately after the gadolinium injection a total of approximately 100,000 microspheres were injected into the circulation at the same site used for gadolinium injection. Up to 3 different colours of microspheres were used during the experiments. Quantitative analysis of the microtome images was performed in the same standard segments used for perfusion quantification according to previously described methods [21]. Flow was calculated in ml/gr/min of tissue from the following equation:

$$\frac{N_S}{M_S} \times \frac{F_t}{N_t}$$

Where N_s(the number of microspheres) is counted in a segment, N_t is the total number of injected microspheres, $F_t$is the total arterial input flow rate in ml/min and M_S is the mass of a segment in grams.

3.3 Statistical Analysis

For synthetic data, numerical considered methods were compared by using absolute perfusion error (e_a), which is defined as $e_a = |MBF - MBF_{ref}|$ where MBF_{ref} is the known reference simulated flow value. Mean ±standard deviation (STD) of $e_a$was calculated for each different condition tested in the synthetic data to assess the sensitivity of the methods to varying parameters.The paired samples T-test was used to compare perfusion measurements between different deconvolution methods. To compare CMR perfusion measurements and microspheres, linear regression analysis was used. Coefficient of variation (CV) is calculated to assess dispersion and variation of each algorithm results due to variation in model order.

4 Results

4.1 Simulated Data

Using the four methods, the respective plots of simulated $C_{aif}(t)$ and $C_{myo}(t)$ curves along with the reconstructed $C_{myo}(t)$ curves from deconvolution is shown on the right hand column of figure 1. On the left hand side, each methods corresponding extracted tissue impulse response is demonstrated using the following model orders-cubic B-spline with 5 control points (A), second order autoregressive mode (AR) (B), i.e. Q=0 ,L=2, Exponential with 10 time scales (C) and Fermi (D).

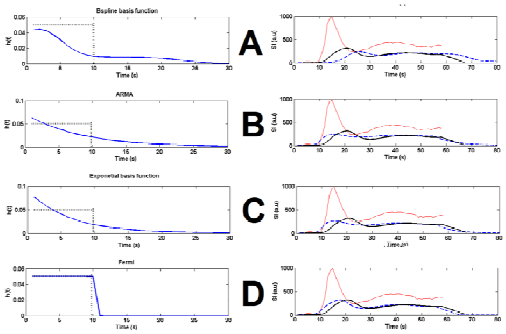

Fig. 1. Results of solving the deconvolution for synthetic data with B-spline(A), ARMA (B), exponential basis function (C) and Fermi (D) function modelling are shown in first , second, third and fourth row respectively. The dashed curve in the left column is the exact synthetic $h(t)$ (step function). The solid blue curves in the left column are the estimation of the tissue impulse response. The slid curves in the right column are simulated tissue and arterial input curve and the dashed lines are convolution of estimated $h(t)$ and $C_{aif}(t)$. Note that Fermi model provides the closest simulated tissue impulse response to real one.

Table 1 represents the modelling parameters of each deconvolution method. These parameters mainly can be divided into two groups: 1) Parameters which will be estimated during deconvolution regularization process (second column), 2) parameters which are independent of the deconvolution process and need to be set (third column). The range of values assigned to these deconvolution independent parameters for investigation is represented in fourth column. These ranges of values are chosen based on the previous studies suggestions [7, 10, 11, 14, 16].

Table 1. Deconvolution methods modelling parameters

Mathematical model	Parameters estimated with deconvolution	Deconvolution independent parameters	Rang of values
B-spline	h_j	$P\ and\ k$	$k = 2{:}4,\ P = 3{:}15$
ARMA	$a_i\ and\ b_j$	$Q\ and\ L$	$Q = 0{:}3,\ L = 1{:}4$
Exponential	h_m	M	$M = 5{:}20$
Fermi	kr, F	τ_{onset}	Not applicable

The deconvolution independent parameter in Fermi modelling, τ_{onset}, is a predefined set parameter which is equal to the delay time between arrival of contrast in LV and myocardium ROI. This parameter is dependent only on each individual ROI and is user independent[18].

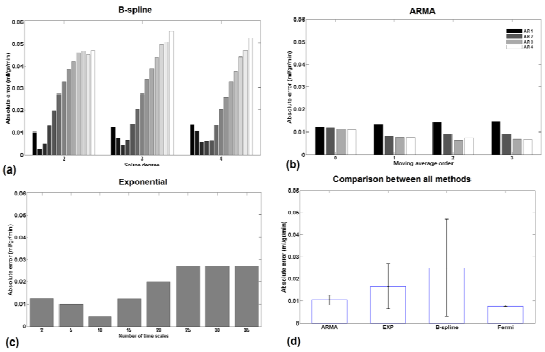

Fig. 2. Bar plots represent the MBF estimates absolute error due to changes in the varying parameters of (a) B-spline, (b) ARMA, (c) exponential. Fermi function method have been compared to mean and SD of all configurations for the synthetic data (d).

The bar plots in figure 2 represents the *MBF* estimates absolute errors (e_a) for B-spline (a), ARMA (b), exponential (c) –due to changes in the varying parameters as mentioned in table 1. For B-spline method more accuracy was achieved when a smaller number of control points was used for modelling ($P = 5,\ e_a = 0.004, 8\%$). For the same number of used control points, all degrees of splines had almost similar level of accuracy. For the exponential model the best accuracy was achieved with $M = 10$ ($e_a = 0.004, 9\%$). All auto regressive model orders in absence of a moving

average model (i.e $L = 1{:}\,4$ where $Q = 0$) provided accurate and reliable estimates. However when the moving average part (MA) is added to the model, ARMA with a higher AR order achieved a better accuracy (figure 2.b). Compared to all models, the Fermi function was most accurate with an absolute error equal to 0.0035 (figures 2.d).

Table 2 represents the coefficient of variation (CV) for each deconvolution model varying parameters. For an AR model, CV of *L* increases proportionally to the order of MA part. The highest CV belongs to *Q=3(*CV=55%*),* and the lowest belongs to *Q=0 (*CV=4%*).*However for the MA part of ARMA (where AR order (*L*) is constant and MA order (*Q*) varies), *L=1* has the highest CV *(*CV=23%*).* In the B-spline model, variation in order of the splines (*k*) had a CV of 5%, whereas the variation in number of nodes *(P)* had higher CV (58% for *k=3* and 66% for *k=4*). For exponential model time scales (*M*) CV was equal to 40%.

Table 2. Coefficient of variation (CV) of deconvolution models varying parameters for synthetic data

Algorithm /Varying parameter		CV % (std/mean)
B-spline/ *P*	*k*=3	58 %
	k=4	66%
B-spline/*k*		5 %
AR/*L*	*Q=0*	4 %
	Q=1	43 %
	Q=2	50%
	Q=3	55 %
MA/*Q*	*L=1*	23 %
	L=2	16 %
	L=3	17 %
	L=4	18 %
EXP/ *M*		40 %

To determine the number of spline nodes (control points) and exponential basis function time scales, the L-curve approach was adapted from the least square context. A plot of $log\left\|C_{myo} - h * C_{aif}\right\|$ versus $log\|h'\|$ is shown in figure 3.a and 3.b for varying number of regularly spaced B-spline nodes and Exponential time scales, respectively.

Of note, it is important to appreciate that for the examples demonstrated in this work, the number of B-spline nodes which delivers the best match to the exact tissue curve is small. The latter is the same for exponential functions. The higher absolute error demonstrated in fig 2.b (due to overestimation of the initial value) is typical of results achieved with a large number of time scales.

Sensitivity of the ARMA model to order of AR and MA parts has been tested by keeping the orders of one part (for instance AR part) fixed and varying the other part order. In each stage of the process, MBF has been estimated and absolute error has been calculated. Mean and standard deviation of absolute error is represented in figure 4.

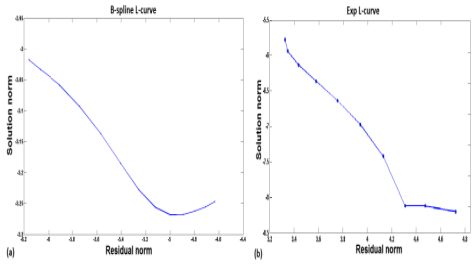

Fig. 3. The L-curves are generated by varying the number of spline nodes (control points) for B-spline (a) and number of time scales for exponential (b) and plotting $log\left\|C_{myo} - h * C_{aif}\right\|$ versus $log\|h'\|$. The number for spline nodes and exponential time scales is associated with the first point where a local minimum is detected in the angle subtended at a vertex in L- curve.

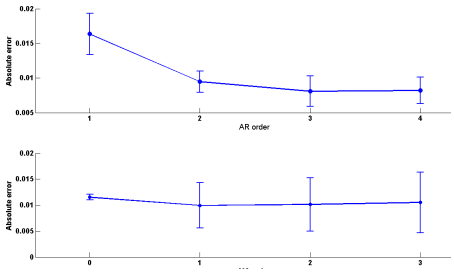

Fig. 4. Error bars represents means and standard deviation of the ARMA method MBF estimates absolute error for (a) fixed auto regressive (AR) orders while moving average (MA) order varies and (b) fixed MA orders while the AR order varies. Note that AR absolute error decreases as the order of AR falls down whereas for the MA model absolute error remains almost constant.

Error bars in figure 4.a represent the e_a and STD of different orders of AR model due to variation in Q (order of MA part of ARMA model). First order AR has the highest error and STD amongst all. Second order AR had the lowest STD. In figure (4.b) the e_a and STD of MA part of ARMA is represented. Whilst all MA orders have similar level of accuracy, MA with Q=0 had the lowest STD. STD increases as MA order increases.

4.2 Explanted Perfused Pig Heart

In this section the relationship between microspheres and the average perfusion values, derived from the four respective different techniques based on CMR SI-time curves were examined. The correlation coefficient values (r^2) have then been summarized in table 3. From the correlation coefficients the following four interpretations can be derived. Firstly, the high r^2 values close to 1 suggest that there is a good correlation between all CMR derived MBF estimates and the microspheres. Secondly, third order AR model with constrained deconvolution achieved the best correlation ($r^2 = 0.926, \mathrm{p} < 0.001$) whilst the exponential basis function deconvolution with $M = 15$ resulted in the weakest correlation ($r^2 = 0.539, \mathrm{p} < 0.001$). Thirdly, for

ARMA model correlation with microspheres was stronger when the order of the AR part was stronger than the MA part ($r^2 = 0.833$ to 0.926). Fourthly, correlation was stronger for Fermi ($r^2 = 0.911$) and ARMA model compare to B-spline and exponential basis model.

The pig heart relative MBF error:

$$e_{rel} = \frac{|\text{CMR delivered perfusion values} - \text{microspheres}|}{|\text{CMR delivered perfusion values}|} = \frac{e_a}{|MBF|}$$

is represented in figure 5 as bar plots. Analysis show excellent result for Fermi deconvolution with small error in estimation of perfusion ($e_{rel} = 0.21$). AR model with ($L = 2$, 3) and ARMA with ($L = 2$, $Q = 1$) had almost similar level of accuracy as Fermi model. Exponential deconvolution showed excellent results at $M=5$ ($e_{rel} = 0.21$) and $M=10$ ($e_{rel} = 0.19$). B-spline deconvolution showed high accuracy in flow estimation for $P=5$ and 10 ($e_{rel} = 0.21$).

Table 3. The table shows the correlation strength of the individual algorithms order with microspheres

Algorithm		r^2
AR	**L=1**	.740
	L=2	.897
	L=3	.926
	L=4	.872
ARMA Q=1	**L=1**	.85
	L=2	.920
	L=3	.890
	L=4	.890
ARMA Q=2	**L=1**	.780
	L=2	.833
	L=3	.903
	L=4	.843
FERMI		.911
EXP	**M=5**	.860
	M=10	.885
	M=15	.539
	M=20	.657
B-spline *k*=3	**P=5**	.836
	P=10	.731
	P=15	.764
B-spline *k*=4	**P=5**	.877
	P=10	.793
	P=15	.748

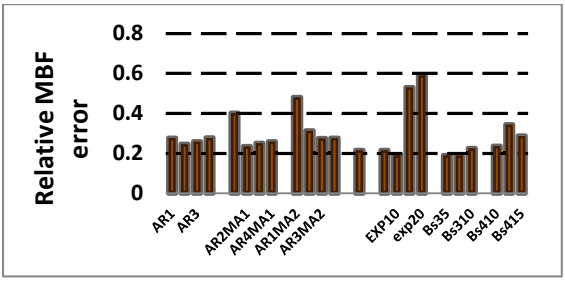

Fig. 5. The bar plots represents relative MBF error for the explanted pig heart

5 Discussion

Modelling of systems typically proceeds by adopting a class of systems capable of producing the observed outputs and having a structure compatible with our prior knowledge of the nature of the system or source. The problem of model order estimation is one of determining the number and value of the real parameters required to characterize a system.

In this paper we have addressed the issue of the determination of the dimension of the parameters characterizing the myocardial tissue impulse response.

This study has two points of strength. First of these is utilisation of simulated synthetic data with known tissue impulse response, which has allowed us to examine the accuracy and precision of different model orders. The second is the existence of a very controlled animal environment where myocardial blood flow to the heart is known and its distribution over time within the myocardium is quantified with CMR and validated versus microspheres. In this study, the relationship between the estimated perfusion values and the true perfusion values for all four fully quantitative methods with different orders are reported. In general , the low perfusion estimation absolute error in both synthetic simulated data and pig heart and the good correlation between the CMR derived perfusion estimates assessed with either Fermi, ARMA, Exponential basis or B-spline basis deconvolution and the fluorescent-labeled microspheres demonstrate the reliability of the quantification methods for MBF estimation.

While, Fermi function modelling had the lowest average absolute error amongst all methods, B-spline model with 5 control points ($P=5$), second and third order AR, ARMA with ($L=2,Q=1$) and exponential basis with $M=10$ showed to have similar or better accuracy compare to Fermi function modelling. Amongst all four deconvolution algorithms, Fermi function modelling is favourable for its rigidity and independency from modelling parameter determination, whereas all other methods accuracy and precision showed to be very dependent on the modelling parameter. The high value of coefficient of variation for B-spline total number of control points (P) in synthetic data shows its sensitivity to total number of break points. While the degree of piecewise linear spline functions seems not to be very important factor in accuracy of the deconvolution results.

L-curve approach, statistical analysis and the correlation results in both synthetic data and explanted pig heart recommend that the total numbers of nodes which deliver the best match to the exact kernel and give the most accurate results for B-spline basis deconvolution are rather small. The modelling parameter variation sensitivity for exponential basis deconvolution in synthetic data was an inverted bell shape with the local minimum at $M=$. Choosing a value large or smaller than this value will lead to over estimation or under estimation of the initial value of the tissue impulse response, respectively. Our investigation demonstrated that the accuracy of the ARMA models it highly depend on the order of MA part of the ARMA (i.e Q). For $Q=0$, all AR orders (L) showed to have almost similar accuracy. When $Q>0$, the impact of the AR order on perfusion estimation accuracy increases. For noiseless clean data and when $Q>0$, higher AR orders archived better accuracy compare to low order AR models. Whereas for noisy data (which is the case for CMR perfusion assessment), the lower AR orders showed to be more accurate. An explanation, in the simplest sense, for this behavior of ARMA model would the number of poles used for the system transfer function characterization (AR order). In fact by using smaller AR orders, we are using less exponential function to model the tissue impulse response and thus we increase the system degree of the freedom and smoothness. As a result ARMA model will be able to model the system more accurately. Furthermore the values of the poles and the zeros of a system determine how well the system performs. Physically realisable proper systems must have a number of poles greater than or equal to the number of zeros $(L \geq Q)$. Any system with number of zeros greater than pole would deliver output signals of arbitrary high amplitude for input signals of arbitrary high frequency, which are physically not realisable. (i.e. $H(z) \to \infty \ as \ z \to \infty$). A *proper* transfer function always follows $H(z) \to \lambda \ as \ z \to \infty$. Therefore for ARMA model to be realisable and accurate, the order of AR should be greater than the order of MA part. Our investigations demonstrated that for ARMA Model, a strictly proper transfer function ($L>Q$) will result in more accurate estimation of MBF. The best results have been achieved with second and third order autoregressive ($L=2, 3$) and with ($L=2, Q=1$). With reference to given evidences above, we believe that ARMA model with the correct choice of order is clearly superior to other methods with higher correlation coefficients, better accuracy and less computational burden.

Limitations: The fact that the explanted heart is less physiological and free from external influences such as heart rate and cardiac output makes it an ideal validation platform for quantitative perfusion. However this model oversimplifies in vivo physiological conditions with complex nervous cardiac regulation, breathing motion during stress and dilution of contrast in the LV and aorta.

6 Conclusion

Using an appropriate order for quantification algorithms is essential to allow CMR perfusion quantification to develop into a useful clinical tool.

The choice model order depends on several factors including signal to noise ratio of the data, computational burden and desired accuracy of the results. Fermi function modelling was the least dependent method on modelling parameter determination. This characteristic makes Fermi model the most favorable method.

References

1. Ichihara, T., Ishida, M., Kitagawa, K., Ichikawa, Y., Natsume, T., Yamaki, N., Maeda, H., Takeda, K., Sakuma, H.: Quantitative analysis of first-pass contrast-enhanced myocardial perfusion MRI using a Patlak plot method and blood saturation correction. Magn. Reson. Med. 62, 373–383 (2009)
2. Ishida, M., Morton, G., Schuster, A., Nagel, E., Chiribiri, A.: Quantitative Assessment of Myocardial Perfusion MRI. Curr. Cardiovasc. Imaging. Rep. 3, 8 (2010)
3. Zierler, K.: Indicator dilution methods for measuring blood flow, volume, and other properties of biological systems: a brief history and memoir. Annals of Biomedical Engineering 28, 836–848 (2000)
4. Jerosch-Herold, M.: Quantification of myocardial perfusion by cardiovascular magnetic resonance. J. Cardiovasc. Magn. Reson. 12, 57 (2010)
5. Engl, H.W., Hanke, M., Neubauer, A.: Regularization of inverse problems. Kluwer Academic Publishers, Dordrecht (1996)
6. Gill, P.E., Murray, W., Wright, M.H.: Practical optimization. Academic Press, London (1981)
7. Keeling, S.L., Kogler, T., Stollberger, R.: Deconvolution for DCE-MRI using an exponential approximation basis. Medical Image Analysis 13, 80–90 (2009)
8. Pack, N.A., DiBella, E.V., Rust, T.C., Kadrmas, D.J., McGann, C.J., Butterfield, R., Christian, P.E., Hoffman, J.M.: Estimating myocardial perfusion from dynamic contrast-enhanced CMR with a model-independent deconvolution method. J. Cardiovasc. Magn. Reson. 10, 52 (2008)
9. Pack, N.A., DiBella, E.V.: Comparison of myocardial perfusion estimates from dynamic contrast-enhanced magnetic resonance imaging with four quantitative analysis methods. Magn. Reson. Med. 64, 125–137 (2010)
10. Zarinabad, N., Chiribiri, A., Hautvast, G.L., Ishida, M., Schuster, A., Cvetkovic, Z., Batchelor, P.G., Nagel, E.: Voxel-wise quantification of myocardial perfusion by cardiac magnetic resonance. Magnetic Resonance in Medicine: Official Journal of the Society of Magnetic Resonance in Medicine / Society of Magnetic Resonance in Medicine 68, 1994–2004 (2012)
11. Jerosch-Herold, M., Swingen, C., Seethamraju, R.T.: Myocardial blood flow quantification with MRI by model-independent deconvolution. Med. Phys. 29, 886–897 (2002)
12. Jerosch-Herold, M., Wilke, N., Stillman, A.E.: Magnetic resonance quantification of the myocardial perfusion reserve with a Fermi function model for constrained deconvolution. Med. Phys. 25, 73–84 (1998)
13. Batchelor, P., Chiribiri, A., Nooralipour, N.Z., Cvetkovic, Z.: Arma Regularization of Cardiac Perfusion Modeling. In: International Conference on Acoustics, Speech and Signal Processing, ICASSP 2010, pp. 642–645 (2010)
14. Neyran, B., Janier, M.F., Casali, C., Revel, D., Canet Soulas, E.P.: Mapping myocardial perfusion with an intravascular MR contrast agent: robustness of deconvolution methods at various blood flows. Magn. Reson. Med. 48, 166–179 (2002)
15. Wang, L., Jerosch-Herold, M., Jacobs Jr., D.R., Shahar, E., Folsom, A.R.: Coronary risk factors and myocardial perfusion in asymptomatic adults: the Multi-Ethnic Study of Atherosclerosis (MESA). J. Am. Coll. Cardiol. 47, 565–572 (2006)
16. Hautvast, G., Chiribiri, A., Zarinabad, N., Schuster, A., Breeuwer, M., Nagel, E.: Myocardial blood flow quantification from MRI by deconvolution using an exponential approximation basis. IEEE Transactions on Bio-medical Engineering 59, 2060–2067 (2012)

17. Wilke, N., Jerosch-Herold, M., Wang, Y., Huang, Y., Christensen, B.V., Stillman, A.E., Ugurbil, K., McDonald, K., Wilson, R.F.: Myocardial perfusion reserve: assessment with multisection, quantitative, first-pass MR imaging. Radiology 204, 373–384 (1997)
18. Zarinabad, N., Hautvast, G., Breeuwer, M., Nagel, E., Chiribiri, A.: Effect of tracer arrival time on the estimation of the myocardial perfusion in DCE-CMR. Journal of Cardiovascular Magnetic Resonance 14, 16 (2012)
19. Shuster, A.: Validation of Quantitative Myocardial Perfusion Magnetic Resonance Imaging. Division of imaging sciences and biomedical engineering, ph.D. King College London, London (2012)
20. Ishida, M., Schuster, A., Morton, G., Chiribiri, A., Hussain, S., Paul, M., Merkle, N., Steen, H., Lossnitzer, D., Schnackenburg, B., Alfakih, K., Plein, S., Nagel, E.: Development of a universal dual-bolus injection scheme for the quantitative assessment of myocardial perfusion cardiovascular magnetic resonance. J. Cardiovasc. Magn. Reson. 13, 28 (2011)
21. van Horssen, P., Siebes, M., Hoefer, I., Spaan, J.A., van den Wijngaard, J.P.: Improved detection of fluorescently labeled microspheres and vessel architecture with an imaging cryomicrotome. Med. Biol. Eng. Comput. 48, 735–744 (2010)